

A Comparison of Low-Cost Collector Configurations for Quantifying Ice Accretion

JOHN L. CAMPBELL,^a LINDSEY E. RUSTAD,^a SARAH GARLICK,^b NOAH NEWMAN,^c
JOHN S. STANOVICK,^d IAN HALM,^e CHARLES T. DRISCOLL,^f BRIAN L. BARJENBRUCH,^g
ELIZABETH BURAKOWSKI,^h STEVEN D. HILBERG,^c KRISTOPHER J. SANDERS,ⁱ JASON C. SHAFER,^j AND
NOLAN J. DOESKEN^c

^a USDA Forest Service Northern Research Station, Durham, New Hampshire

^b Hubbard Brook Research Foundation, Woodstock, Vermont

^c CoCoRaHS, Colorado Climate Center, Colorado State University, Fort Collins, Colorado

^d USDA Forest Service Northern Research Station, Newtown Square, Pennsylvania

^e USDA Forest Service Northern Research Station, North Woodstock, New Hampshire

^f Department of Civil and Environmental Engineering, Syracuse University, Syracuse, New York

^g NOAA/National Weather Service, Valley, Nebraska

^h Institute for the Study of Earth, Oceans, and Space, University of New Hampshire, Durham, New Hampshire

ⁱ NOAA/National Weather Service, Grand Junction, Colorado

^j Department of Atmospheric Sciences, Northern Vermont University, Lyndon, Vermont

(Manuscript received 20 November 2019, in final form 17 July 2020)

ABSTRACT

Ice storms are important winter weather events that can have substantial environmental, economic, and social impacts. Mapping and assessment of damage after these events could be improved by making ice accretion measurements at a greater number of sites than is currently available. There is a need for low-cost collectors that can be distributed broadly in volunteer observation networks; however, use of low-cost collectors necessitates understanding of how collector characteristics and configurations influence measurements of ice accretion. A study was conducted at the Hubbard Brook Experimental Forest in New Hampshire that involved spraying water over passive ice collectors during freezing conditions to simulate ice storms of different intensity. The collectors consisted of plates composed of four different materials and installed horizontally; two different types of wires strung horizontally; and rods of three different materials, with three different diameters, and installed at three different inclinations. Results showed that planar ice thickness on plates was 2.5–3 times as great as the radial ice thickness on rods or wires, which is consistent with expectations based on theory and empirical evidence from previous studies. Rods mounted on an angle rather than horizontally reduced the formation of icicles and enabled more consistent measurements. Results such as these provide much needed information for comparing ice accretion data. Understanding of relationships among collector configurations could be refined further by collecting data from natural ice storms under a broader range of weather conditions.

KEYWORDS: Ice thickness; Icing; Instrumentation/sensors; Measurements; Surface observations; Icing

1. Introduction

Ice storms are an important natural hazard in many regions of the world (Zhou et al. 2011; Groisman et al. 2016; Nagel et al. 2016). Freezing-rain events commonly occur when a warm, saturated layer of air in the atmosphere overrides a shallow layer of subfreezing air at ground level (Stewart and King 1987; Gay and Davis 1993; Rauber et al. 2001; Cortinas et al. 2004). Frozen precipitation falling into the warm layer melts and then subsequently supercools as it passes through the cold

layer and freezes when deposited to subfreezing surfaces. Freezing rain and drizzle can also form through the supercooled warm-rain process (Huffman and Norman 1988; Rauber et al. 2000), which occurs in the absence of a warm layer of air. If freezing nuclei (i.e., ice crystals and aerosols) are lacking in partially or wholly subfreezing clouds (usually from -10° to 0°C), water droplets remain in the liquid phase. The water droplets collide and coalesce as they descend through the cloud and stay in a supercooled state until reaching subfreezing surfaces where they form ice.

The glaze ice that accumulates during ice storms can be highly destructive, damaging forests and tree crops,

Corresponding author: John Campbell, john.campbell2@usda.gov

impairing infrastructure, disrupting services, and causing vehicle collisions that result in injuries and fatalities (DeGaetano 2000; Irland 2000; Changnon 2003; Changnon and Creech 2003; Call 2010; Zhou et al. 2011; Tobin et al. 2019). In the United States, ice-storm damage averages \$313 million per year (Zarnani et al. 2012), with some individual storms exceeding \$1 billion (Smith and Katz 2013). The northeastern region of the United States has the greatest risk of ice-storm damage, based on event frequency, ice thickness, storm size and shape, and financial loss (Changnon 2003). Recent increases in freezing-rain events reported in the Midwest and areas north suggest that the spatial distribution of freezing rain may be shifting in the United States; however, more data are needed to determine whether these patterns are due to natural variability or to longer-term changes in climate (Landolt et al. 2019).

Many different types of automated sensors have been developed to detect ice accretion (Homola et al. 2006; Virk et al. 2011; Mughal et al. 2016). Although these sensors have improved over time, they still have limitations, such as large electrical power requirements for heated devices, difficulties discerning precipitation type, and challenges in maintaining operability during icy conditions (Mughal et al. 2016). Some of these sensors are designed to measure ice loads on structures in accordance with standards developed by the International Organization for Standardization (ISO; ISO 2017). The ISO recommends an ice measuring device consisting of a smooth, 30-mm-diameter rotating cylinder that is oriented vertically and is at least 0.5 m long. However, these sensors are not appropriate in all applications and under all conditions. Moreover, some countries, such as the United States, have adopted alternative standards.

In the United States, the National Weather Service (NWS) has freezing-rain sensors located at more than 650 of the more than 900 sites composing the Automated Surface Observing System (ASOS) network (<https://www.weather.gov/asos/>; Sanders and Barjenbruch 2016). This network serves as the country's primary source of climatological data, and ASOS sensor arrays are often installed at airports to inform aviation activities as well as other meteorological applications. These sensors detect the presence of freezing rain through measurement of frequency change on a vertically oriented vibrating rod, rather than directly measure ice accretion. However, algorithms have been developed to convert frequency change to ice accretion based on manual measurements of ice thickness and mass (Tattelman 1982; Ryerson and Ramsay 2007). Despite the advantages that these sensors provide, the model approved for use in the ASOS network is costly (\$13,000), and other lower-priced sensors

(Mughal et al. 2016) are still too expensive for widespread deployment.

In addition to sensor-based measurements, numerous models have been developed to simulate ice accretion on surfaces (e.g., Jones 1998; Makkonen 2000; Myers and Charpin 2004; Szilder 2018). Like sensors, these models have improved over time; however, they require meteorological inputs for simulation, and in some cases rely on data that are not commonly collected, such as droplet size and liquid water content. Estimates of ice from both models and sensors could be tested more rigorously and improved with direct, manual, field-based observations of poststorm ice accretion.

Networks of passive ice collectors have been established in some countries, usually for specific purposes, such as estimating ice loads on electrical transmission lines and towers (Laflamme 1995; Fikke et al. 2006). In the United States, some manual measurements of glaze ice have been made for various periods by national associations and businesses including electric power, telephone, and railroad, whose operations are impacted by ice storms (Bennett 1959; Changnon and Creech 2003; Changnon and Karl 2003). Most recently, ice accretion has been included as an optional measurement in the Community Collaborative Rain, Hail and Snow Network (CoCoRaHS; <https://www.cocorahs.org>), a climate observation network composed of citizen scientists primarily in the United States and Canada, who make daily measurements of rain, hail, and snow, and report them online (Cifelli et al. 2005; Reges et al. 2016). The network currently consists of 26 000 sites, many of which are in areas affected by freezing rain (Fig. 1). Although CoCoRaHS encourages observers to record ice accretion amounts and provides some suggestions of how to make measurements (https://media.cocorahs.org/docs/Training_IceAccretion.pdf), the network has not yet adopted a routine, standardized approach.

Comparing measurements of ice accretion obtained with different methods can be challenging. Previous research has demonstrated that ice accretion can vary on different surfaces (Poots 1996); however, more information is needed on how collector configurations affect ice accretion values. Better understanding of relationships in ice accretion among collector types will improve our ability to compare observations within and across networks. Inclusion of ice accretion observations in citizen scientist networks requires equipment that is inexpensive and easy to install and maintain. Measurements should be straightforward to make and interpret. This study evaluates proof-of-concept designs for low-cost ice collectors for potential use by citizen scientists. The major goals of this study were to 1) test passive ice collector designs to inform decisions about how best to

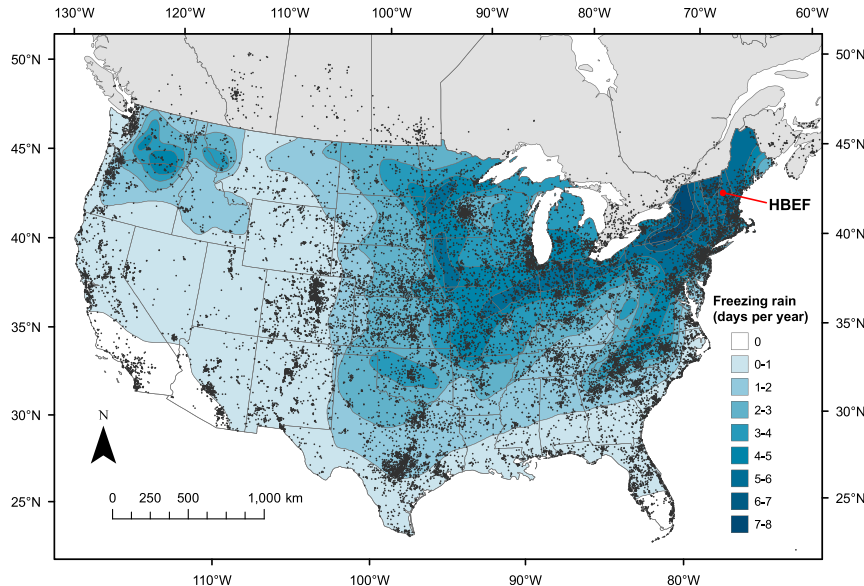


FIG. 1. CoCoRaHS network observer locations (black circles) in the conterminous United States and southern Canada. Shading indicates the average annual number of days with freezing rain in the United States from Changnon (2003). The location of the HBEF is indicated in red.

collect ice measurements, 2) provide information that improves the ability to interpret ice accretion data obtained with different collector configurations, and 3) assess the repeatability of ice thickness measurements. Improvements in the quality and usability of ice accretion data will enable scientists, weather observers, emergency personnel, and others to better evaluate ice storms and their impacts.

2. Materials and methods

a. Experimental design

In this study, ice accretion measurements were made on solid rods, flat plates, and wires. We compared ice accretion on rods of three diameters [19.1 mm (0.75 in.), 25.4 mm (1 in.), and 31.8 mm (1.25 in.)], composed of three materials [wood, dark-gray polyvinyl chloride (PVC), and aluminum], and mounted at three inclinations [0° (i.e., horizontal), 30° , and 60°]. The materials used (i.e., wood, PVC, and aluminum) were selected on the basis of their wide availability, range of thermal properties and durability, and relatively inexpensive cost. We did not include vertically oriented rods in this study because unheated, vertically oriented rods have been shown to be inappropriate for quantifying glaze ice formed through the wet growth process because of poor adherence (Virk et al. 2011, 2015). Each rod was 60 cm long and attached to one side of a post (i.e., one rod per side and four rods per post) using two galvanized steel

two-eyed straps (Fig. 2a). The posts were 9 cm \times 9 cm and installed at a height of 1.2 m above the ground.

Plates (10 cm \times 30 cm \times 0.6 cm) were constructed of three different materials (plywood, aluminum, and PVC) and glued with construction adhesive to a 1.3-cm-thick marine-grade plywood base (Fig. 2b). The PVC plates were two different colors (white and dark gray) but otherwise were identical. Each of the four different types of plates (wood, white PVC, gray PVC, and aluminum) was mounted horizontally with a shelf bracket on posts that were identical to those used for rods (four plates per post).

Ice accretion on wires was determined with two types of electrical transmission lines: 1) a bare neutral wire that consisted of 8-mm-diameter stranded aluminum conductor steel-reinforced cable (six 2.7-mm aluminum wires wrapped around one 2.7-mm steel wire) and 2) an insulated phase wire that consisted of 9.7-mm-diameter stranded all aluminum conductor cable (seven 2.5-mm aluminum wires) covered with a 1.1-mm-thick layer of black cross-linked polyethylene.

One-meter lengths of each wire type were suspended horizontally 1 m above the ground between posts with mounted rods or plates. The 1-m wires were centered between posts and attached with U bolts to two 0.5-m lengths of smaller wire on both ends to make up the 2-m span (Figs. 2a,d).

Twelve posts were arranged in a grid (3 posts \times 4 posts with 2-m spacing between posts) in each of two adjacent

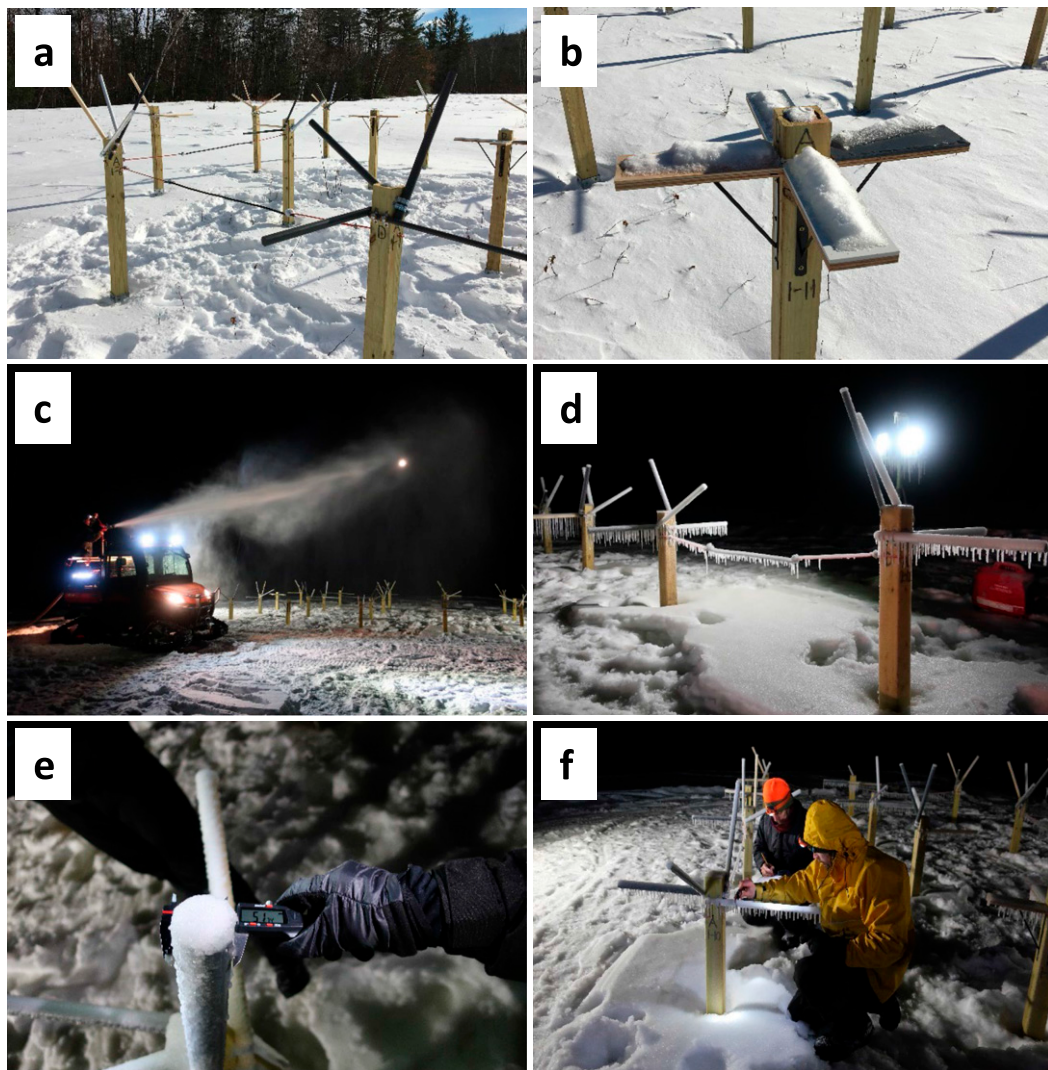


FIG. 2. (a) Ice collectors consisting of rods, wires, and plates; (b) plates with snow that was removed before the ice addition; (c) spraying water over the collectors to simulate an ice storm; (d) ice accumulation on rods and wires after the lower ice application; (e),(f) measuring ice accretion with calipers. The photographs in (a) and (b) were taken by J. Campbell, and those in (c)–(f) are provided through the courtesy of C. Chaisson.

blocks (24 posts total; [Fig. 3](#)). Twenty of the posts were used for ice measurements on rods, and four posts were used for ice measurements on plates. Posts were randomly selected to have either rods or plates, and each side of the posts was randomly assigned a specific type of rod or plate. Wires were randomly assigned to pairs of adjacent posts. There were from two to four replicates of each unique rod combination (i.e., diameter, inclination, and material), four replicates of each plate material, and three replicates of both wire types.

b. Site description

The study was conducted in an open field in front of the Robert S. Pierce Ecosystem Laboratory at the

Hubbard Brook Experimental Forest (HBEF; [Fig. 1](#)) in central New Hampshire ($43^{\circ}56'36''\text{N}$, $71^{\circ}41'58''\text{W}$). The climate at the HBEF is cool, humid, and continental with an average monthly low air temperature of -9°C in January and a high of 18°C in July ([Campbell 2016](#)). Mean annual precipitation is 1400 mm and is distributed evenly throughout the year, with approximately one-third falling as snow ([USDA Forest Service, Northern Research Station 2019](#)). Hubbard Brook is in a region of the United States that receives an average of 5–6 days of freezing rain annually ([Changnon 2003](#)), although the majority of freezing-rain events do not meet the criteria of an ice storm as defined by the NWS [i.e., ice accumulation of 6.4 mm (0.25 in.) or more on an elevated

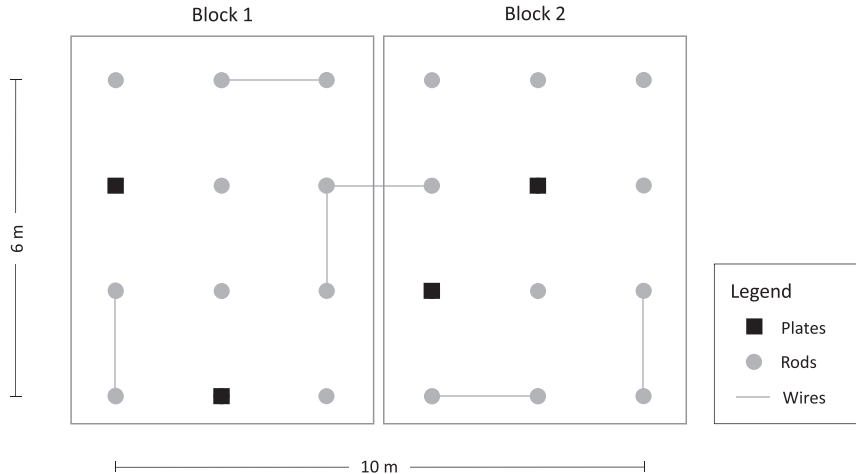


FIG. 3. Schematic of the experimental design showing locations of plates, rods, and wires as viewed from above.

horizontal flat surface; [NWS 2019](#)]. Major ice storms do occur at the site though, the most notable of which was the ice storm of 1998. That storm impacted much of the northeastern United States and southeastern Canada ([DeGaetano 2000](#); [Gyakum and Roebber 2001](#)), producing as much as 125 mm of radial ice thickness (caliper measurements) in some areas ([Jones and Mulherin 1998](#)), and up to 14 mm was measured on branches at the HBEF ([Rhoads et al. 2002](#)). The effects of the storm on forests were substantial and well documented at the HBEF (e.g., [Rhoads et al. 2002](#); [Houlton et al. 2003](#); [Likens et al. 2004](#)) and across the broader region (e.g., [Irland 1998](#); [Jones and Mulherin 1998](#)).

c. Ice-storm simulation and measurement

In lieu of waiting potentially years for ice storms of different intensity to occur, we created an artificial ice storm to make comparisons among collectors (see [Rustad and Campbell 2012](#)). We simulated a glaze ice event by spraying water over the ice collectors during subfreezing conditions ([Figs. 2c,d](#)). Water was pumped from a nearby pond through a 3.8-cm-diameter high pressure firefighting hose and sprayed at a rate of 300 L min^{-1} with a variable stream nozzle. A supply pump was placed next to the pond, and a secondary pump was secured to the bed of a utility task vehicle (UTV). The hose was connected to the pumps and stabilized with a monitor mounted on the UTV. The UTV was driven slowly back and forth alongside the icing study area while water was sprayed evenly over the collectors so that the water droplets fell from above and froze on contact. Two target ice amounts were selected: 6.4 mm (0.25 in.) and 12.7 mm (0.5 in.) of radial ice accretion, hereinafter respectively referred to as “lower”

and “higher” ice treatments. These values were chosen to represent levels of ice accretion that are realistic for major ice storms in the region, such as the ice storm of 1998, which deposited a maximum of 14 mm of ice at the HBEF ([Rhoads et al. 2002](#)).

The ice-storm simulation occurred on 19 February 2019 and the collectors were sprayed and measured at night (from 1830 to 2330 local time) when air temperatures were below freezing. During the simulation, the range in air temperature was from -12° to -10°C , the wet-bulb temperature range was from -13° to -12°C , relative humidity was 51%–64%, and wind speed was less than 1.7 m s^{-1} . Ice thickness measurements were made using digital calipers (Clockwise Tools, Inc., Vinca DCLA-0605) with a manufacturer-specified accuracy of $\pm 0.02 \text{ mm}$. As the ice was being applied, we made periodic random spot measurements with calipers on various collector types (rods and wires) to determine whether the target levels of radial ice thickness were being approached and when to stop spraying. Once the target level of ice had roughly been achieved, we started making the formal measurements used in our analyses. Eighty minutes of spraying was required to reach the lower target level of ice (6.4 mm), at which time we made a round of measurements. We then immediately resumed spraying and continued for another 75 min until reaching the higher target level of ice (12.7 mm), at which time we made two back-to-back rounds of measurements to assess reproducibility as subsequently described in [section 2d](#) (statistical analyses).

Ice accretion on rods and wires was measured both vertically (measured from top to bottom of rod or wire) and horizontally (measured from side to side of rod or wire) at three locations along each rod or wire:

the center location and halfway between the center and the two different ends of the rod or wire (Figs. 2e,f; six measurements per rod or wire). Ice measurements on plates were made at the midpoint of each side, excluding the side that abutted the post (three measurements per plate). Any ice that formed underneath the plates was scraped off prior to making measurements so that only ice that accumulated on top of the plates was measured.

Measurements were made before any ice was applied, and immediately after both levels of icing. In total, 2256 caliper measurements were made in this study: four rounds of measurements (one round without ice, one round for the lower level of ice, and two rounds for the higher level of ice), 480 measurements for rods per round (20 posts, four rods per post, and six measurements per rod), 48 measurements for plates per round (four posts, four plates per post, and three measurements per plate), and 36 measurements for wires per round (six wires, with six measurements per wire).

d. Statistical analyses

Ice measurement data were analyzed with a generalized linear mixed model (the “GLIMMIX” procedure in SAS 9.2; [SAS Institute 2012](#)) fitted with a pseudolikelihood estimation technique. For plates, a nested randomized complete block design was used with level of ice, material (wood, white PVC, gray PVC, and aluminum), and associated interactions as fixed effects, and three random effects: block, post nested within block, and side of post nested within post and block. The data for plates were modeled with a gamma distribution and logarithmic link function. To evaluate the uniformity of ice accumulation on plates, we compared ice thickness measured on each side of the plate using the model described previously, but with measurement position included as an additional fixed effect in the model.

For wires, a randomized complete block design was used with level of ice (lower or higher), wire type (bare aluminum or insulated), and associated interactions as fixed effects, and two-post combinations as a random effect. The data for wires were modeled with a normal distribution and identity link function. To evaluate uniformity of radial ice on wires, we compared horizontal and vertical measurements by including measurement orientation as an additional fixed effect in the model. We also made comparisons of ice thickness at the three measurement positions along the length of the wire by adding measurement position as an additional fixed effect in the model.

For rods, a nested randomized incomplete block design was used with level of ice, rod material (wood, PVC, and aluminum), diameter (19.1, 25.4, and 31.8 mm), inclination (0°, 30°, and 60°), and associated interactions as

fixed effects, and three random effects: block, post nested within block, and side of post nested within post and block. The ice thickness data for rods were modeled with a gamma distribution and log link function. Similar to the statistical method for wires, we compared radial ice uniformity on rods by including measurement orientation (vertical, horizontal) as a fixed effect in the model and compared ice thickness at the three measurement positions along the length of the rod by adding measurement location as a fixed effect.

The Shapiro–Wilk test ([Shapiro and Wilk 1965](#)) was used to ensure that data met the assumption of normality, and Levene’s test ([Levene 1960](#)) was used to evaluate homogeneity of variance. In all models, denominator degrees of freedom were adjusted using the Kenward–Roger approximation. Post hoc analyses were conducted using the Tukey–Kramer test ([Kramer 1956](#)), and differences were considered to be significant at $\alpha = 0.05$.

Measurements made at the higher ice level were repeated to quantify the reproducibility of the data. We did not repeat measurements for the lower ice treatment because of time constraints and chose to repeat measurements for the higher ice treatment because we thought the uncertainty would likely be greater and thus represent the upper bound of uncertainty for the simulation. These blind remeasurement audits were made with different observers but under the same conditions and using the same method. Precision and bias were calculated following the method described by [Hyslop and White \(2009\)](#). Bias is expressed as the scaled relative difference between measurement pairs divided by the mean of measurement pairs using the following equation:

$$\text{Bias}(\%) = 100 \times \frac{1}{n} \sum_{i=1}^n \frac{(x_{i1} - x_{i2})/\sqrt{2}}{\bar{x}_i}.$$

We report precision as coefficient of variation calculated as the root-mean-square of the scaled relative differences between measurement pairs as determined with the following equation:

$$\text{Precision}(\%) = 100 \times \sqrt{\frac{1}{n} \sum_{i=1}^n \left[\frac{(x_{i1} - x_{i2})/\sqrt{2}}{\bar{x}_i} \right]^2}.$$

The 1-standard-deviation estimate of precision (mm) derived from this method provides a range in ice thickness within which the actual thickness is expected to occur 68% of the time.

3. Results

For all three types of collectors, the ice-storm simulation provided two distinct levels of ice thickness for

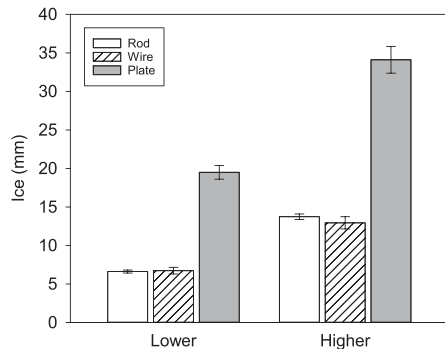


FIG. 4. Comparison of mean ice thickness for rods, wires, and plates for the lower and higher ice applications (i.e., 6.4 and 12.7 mm of ice accretion, respectively). Error bars indicate the standard error of the mean.

analysis. Radial ice thickness measured on rods and wires was close to the target values of 6.4 and 12.7 mm (Fig. 4). Ice thickness on rods and wires amounted to a mean of 6.6 and 6.7 mm and a standard error of 0.2 and 0.4 mm, respectively, for the lower ice treatment. For the higher ice treatment, the respective numbers were 13.7 and 12.9 mm for the mean and 0.4 and 0.8 mm for the standard error. Planar ice thickness on plates was 2.5–3 times that on rods or wires, amounting to a mean and standard error of 19.5 and 0.9 mm, respectively, for the lower ice treatment and 34.1 and 1.7 mm, respectively, for higher ice treatment. The slope of the relationship between radial and planar ice thickness was 0.38, based on the two levels of ice thickness (i.e., a two-point slope).

a. Plates

Results of the generalized linear mixed model for plates confirmed that the treatments produced two distinct levels of ice accretion ($p < 0.001$) that were

representative of the low and high target ice thicknesses. However, there was no significant difference in ice accretion among types of plates (i.e., wood, white PVC, gray PVC, and aluminum; $p = 0.493$) or the interaction of plate type and ice treatment level ($p = 0.778$). There was also no significant difference in accretion among the three locations on the plate where measurements were made ($p = 0.876$).

b. Wires

Similar to plates, statistical analyses for wires indicated a significant difference in ice accretion between the two levels of treatment ($p = 0.007$). However, there was no significant difference in ice accretion between wire types ($p = 0.139$) or the interaction of wire type and treatment level ($p = 0.730$). Vertical measurements were significantly greater than horizontal measurements ($p = 0.040$), indicating that the sum of ice accretion on the top and bottom of wires was significantly greater than the sum of ice accretion on either side of the wires. There was no significant difference in ice accretion among the three positions along the wire where measurements were made; however, the p value was low ($p = 0.099$) and ice accretion tended to be greater at the middle of the wire than at either side of the wire.

c. Rods

For rods, there was a significant interaction between ice treatment level and inclination ($p = 0.010$). At the lower ice treatment level, there was no significant difference in ice accretion between rods positioned at 0° and 30° angles; however, there was significantly less ice accretion on rods positioned at a 60° angle (Fig. 5a). At the higher ice treatment level, ice accretion on rods at a 30° angle was significantly greater than rods at a 0° angle

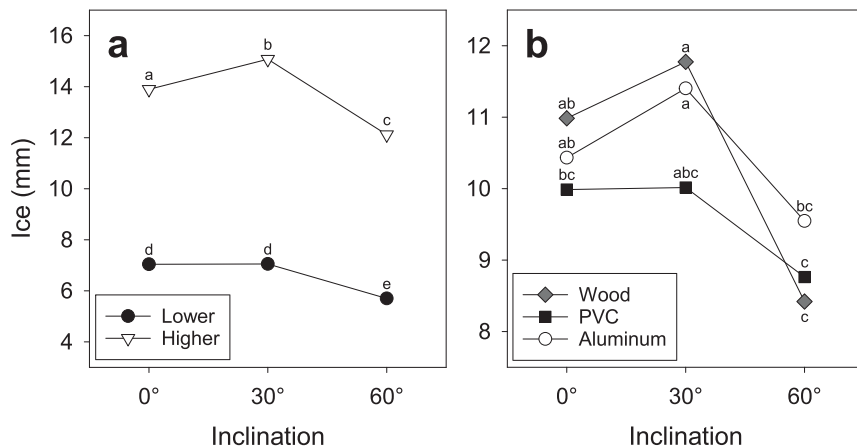


FIG. 5. Ice accretion interactions for rods between inclination and (a) ice treatment or (b) material type of the rods. Nonshared letters indicate significant differences at $\alpha = 0.05$.

followed by rods at a 60° angle. There was also a significant interaction between inclination and material type ($p = 0.035$; Fig. 5b). PVC rods showed no significant difference in ice accretion across all three inclinations. For aluminum rods there was significantly more ice accretion on rods at a 30° angle than rods at a 60° angle. However, there was no significant difference in ice accretion on aluminum rods at a 0° and 30° angle or 0° and 60° angle. Results for wood rods were similar to aluminum in that there was significantly more ice accretion on rods at a 30° angle than rods at a 60° angle, and no significant difference for rods at 0° and 30° angles. However, there was a significant difference in ice accretion between wood rods at 0° and 60° angles. The diameter of the rod (19.1, 25.4, and 31.8 mm) did not significantly affect ice accretion ($p = 0.162$), and none of the other interactions were significant.

We modified the statistical model for rods to compare vertical (top and bottom of rods) and horizontal (sides of rods) caliper measurements of ice accretion. Results showed significant interactions between measurement orientation and inclination ($p < 0.001$), material type ($p < 0.001$), and level of ice ($p = 0.0314$; Fig. 6). Post hoc analyses revealed that for all three inclinations evaluated, vertical ice accretion measurements were significantly greater than horizontal measurements (Fig. 6a). For material types, vertical measurements were significantly greater than horizontal measurements for wood and aluminum, but not for PVC (Fig. 6b). For both levels of ice treatment, vertical measurements were significantly greater than horizontal measurements (Fig. 6c).

Differences in ice accretion at the three measurement locations along the length of rods were also investigated. There was a significant interaction between measurement position and inclination ($p < 0.001$; Fig. 7) but not between measurement position and any of the other effects evaluated (level of ice, rod diameter, material, and inclination).

d. Uncertainty analysis

Uncertainty analyses assessed with duplicate measurements made after the higher level of ice showed a small positive bias ranging from 0.4% on rods to 1.6% on wires (Table 1). As indicated by the coefficient of variation, measurements on wires were the least precise (10.6%) when compared with rods (5.4%) and plates (4.1%). Overall, the standard deviation of ice measurement ranged from 0.7 mm on rods to 1.4 mm on wires and plates.

4. Discussion

a. Weather conditions

The weather conditions (e.g., wet-bulb temperature, wind speed, precipitation rate) during ice storms strongly

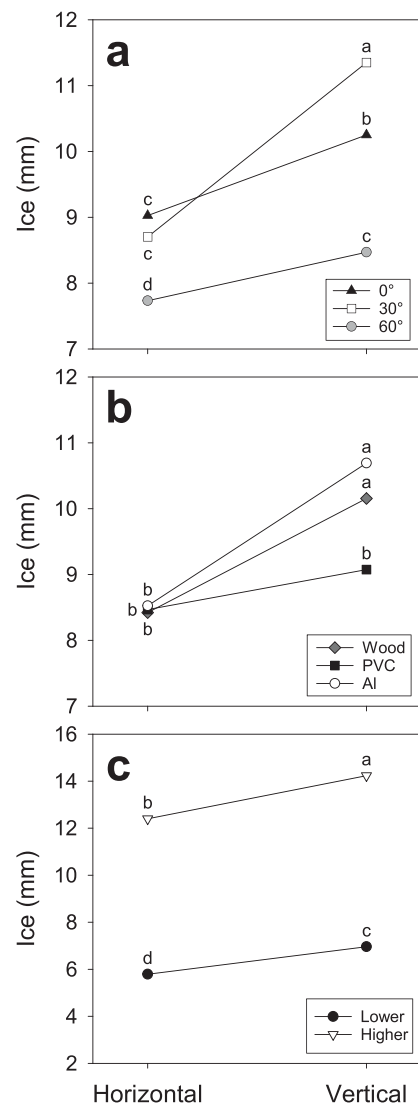


FIG. 6. Ice accretion interactions for rods between measurement orientation and (a) inclination, (b) material type, or (c) ice treatment. Nonshared letters indicate significant differences at $\alpha = 0.05$.

influence the amount and uniformity of ice accretion on objects. Air temperatures in our ice-storm simulation were from -12° to -10°C , as compared with the ice storm of 1998 in which they ranged from -1° to 1°C at the HBEF (Rhoads et al. 2002). Natural ice storms most commonly occur when air temperatures are slightly less than freezing (from -1° to 0°C), and although the temperature during the simulation was colder it is within the temperature range of observed freezing-rain events in the United States (from -15° to 0°C ; Cortinas et al. 2004). We intentionally applied the ice when winds were minimal to prevent drift and to ensure that the spray was distributed evenly over the collectors. Wind speeds during the simulation ($0\text{--}1.7\text{ m s}^{-1}$) were comparable to the

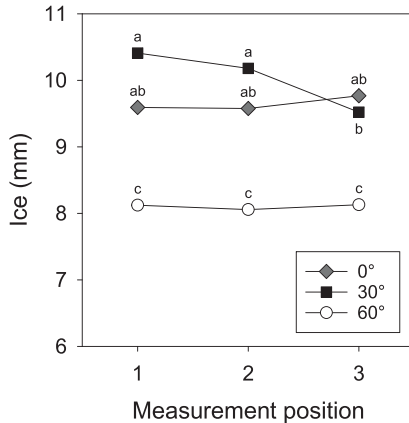


FIG. 7. Ice accretion interaction for rods between measurement position and inclination. Measurement position 1 is closest to the post and is the lowest position on rods installed at 30° and 60°; position 3 is the highest, and position 2 is intermediate. Nonshared letters indicate significant differences at $\alpha = 0.05$.

ice storm of 1998 ($0\text{--}1.3\text{ m s}^{-1}$), but higher wind speeds could impact ice accretion results. Air temperature, wind, and other weather conditions influence how ice forms on collectors as well as other factors such as water droplet size (Ackley and Templeton 1979; Poots 1996; Jones 1998). Water droplet size was not measured in this study; however, the application appeared to be more characteristic of freezing rain than the smaller droplet sizes (less than 0.5 mm in diameter) associated with freezing drizzle and fog (American Meteorological Society 2020). While all three types of freezing precipitation can result in glaze ice, the form influences the rate and shape of ice growth on surfaces (Virk 2017; Poots 1996; Jones 1996). In addition to glaze ice, rime ice can also form when super-cooled water freezes onto surfaces. Rime ice occurs when cloud or fog droplets collide with a surface and freeze rapidly; therefore, it tends to have a lower density and more irregular shape than glaze ice and is not well suited for the measurement approach we used.

Although the ice that accumulated on the collectors in this study was similar in appearance to a natural glaze ice event, the simulation is only representative of one specific set of weather conditions that is not necessarily typical of natural ice storms. It would have been beneficial to repeat the simulation under various weather conditions; however, this was not possible because of logistical and cost constraints. Assessments of ice accretion measurements could be enhanced by collecting data for multiple, natural ice-storm events, but that could take many years at a single site. For example, during the winter of this study, there were no natural ice storms at the study location, except for one minor event that turned from freezing rain to rain, precluding ice accretion measurement. There is a compelling need to

TABLE 1. Uncertainty based on duplicate measurements made after the higher ice treatment, where number of pairs is the total number of duplicate measurements made, bias is the scaled relative difference between measurement pairs divided by the mean of measurement pairs, and precision is the average standard deviation of duplicate measurements expressed as the coefficient of variation and millimeters of ice thickness.

	Rods	Wires	Plates
No. of pairs	480	36	48
Bias (%)	0.4	1.6	1.1
Precision (%)	5.4	10.6	4.1
Precision (mm)	0.7	1.4	1.4

collect standardized, routine data at many locations to cover a broad range of ice accretion under different weather conditions, which will enable better characterization and prediction of ice accretion on surfaces.

b. Collector type

Two distinct levels of ice accretion were produced by the ice-storm simulation. The range in mean radial ice accretion on rods and wires (6.6–13.7 mm) was within the range of measurements obtained after the ice storm of 1998 at the HBEF (0–14 mm; Rhoads et al. 2002). We found substantial differences between planar and radial ice accretion; ice accretion on plates was 2.5–3 times that on rods or wires. This finding is in agreement with expectations that are based on theory as described by Jones (1998). When ice accumulates uniformly on cylindrical objects like rods and wires, the cross-sectional area increases, and the circumference is a factor of π larger than the diameter.

The slope of the relationship between radial and planar ice accretion in our study (0.38) is nearly equivalent to the slope of 0.39 reported by Ryerson and Ramsay (2007) using observations of freezing rain at five sites in the eastern United States. Ryerson and Ramsay (2007) mostly included icing events with less than 20 mm of planar ice, and only one event that was similar to our higher level of icing (i.e., 34 mm). The data for this more extreme event in Ryerson and Ramsay (2007) suggested that the relationship between radial and planar ice may be nonlinear for storms greater than 20 mm since their regression model overpredicted radial ice accretion. However, data from the higher level of icing in our study indicate that the linear relationship is maintained at higher levels of icing. Additional data from other intense ice storms are needed to better characterize this relationship.

The decision of which type of collector to use for measuring ice accretion may be most appropriately determined by the application. For example, plates are more suitable for establishing design loads for buildings

and structures, whereas wood rods mounted on an angle more closely mimic ice loads on tree branches. Installing different types of collectors at the same location, as we have done in this study, improves understanding of relationships in ice accretion among collector types that can be used to refine conversion factors and better establish critical ice load thresholds.

The choice of collector type may also be influenced by the amount of effort it takes to make measurements. Plates require more attention than rods or wires because they accumulate more snow that needs to be removed prior to an ice storm (see Fig. 2b). Although some snow also accumulates on rods and wires, it tends to melt off more rapidly. If snow is removed from plates after each snow event, this issue is less of a problem; however, if snow is allowed to accumulate on the collector, it can turn to ice and become more difficult to remove. Plates also require more effort after an ice storm because icicles that form along the bottom edge of the plates need to be scraped off before measurements are made. This ice can be difficult to remove, especially without disturbing the ice on top of the collector.

c. Collector composition

We compared collectors made of different materials to determine if the composition influenced the amount of ice that accumulated. For plates, the material used (i.e., wood, aluminum, and PVC) did not affect ice accretion. Similarly, the two types of wires evaluated (bare aluminum and insulated) showed no significant difference in ice accretion. It is worth noting that we compared a bare, aluminum neutral wire with an insulated wire that was not conducting electricity. Heat from the current in wires that are actively conducting electricity can reduce ice accumulation, although this “Joule effect” is typically minor (Laforte et al. 1998; Jones et al. 2002). Results from our study are more representative of ice accretion on transmission lines after a power outage or on lines that are otherwise without current. In addition, ice accretion on actual transmission lines may be different than the wires in this study because of the effects of stretching and torsion on lines with longer spans (McComber 1983).

Both wires and plates were installed horizontally, whereas rods were mounted at three inclinations. Results showed a significant interaction between rod material and inclination on ice accretion (Fig. 5b). In general, collectors mounted at the steepest inclination (60°) had less ice, but the difference was only significant for rods composed of wood and aluminum, and not PVC. While these interactions are difficult to interpret, they indicate that material type influenced ice accumulation when collectors were mounted on an angle. It is important to note

that the influence of material type on ice accretion may vary with weather conditions. For example, wood is porous and can absorb water and expand, which may affect ice accretion measurements. The different thermal properties of the materials can also impact the rate of ice accretion.

The diameter of rods did not significantly affect ice accretion as determined by a comparison among rods of three different sizes (19.1, 25.4, and 31.8 mm in diameter). In theory, objects with a larger diameter should accumulate less ice due to a reduction in droplet collision efficiency with the size of the collector (Jones 1996). This relationship has been demonstrated in models (Virk 2017) and under controlled conditions in climate chambers (Makkonen and Stallabrass 1987), although not always (Tattelman 1982), and is strongly influenced by droplet size and wind. What limited field data exist have provided additional evidence for this relationship, which can be described with a power function (Fan and Jiang 2018). Results from our study indicated no relationship, suggesting that any potential effects of rod diameter were masked by other factors, such as airflow around the rods (Fu et al. 2006; Virk 2017).

A comparison of ice accretion on PVC plates of two different colors (dark gray and white) that were otherwise identical showed no significant difference, indicating that there was no albedo effect, which was expected because the ice-storm simulation was conducted at night. However, it is possible that the albedo of the collector could affect the rate of melt in the days and weeks following an ice storm, depending on the incident solar radiation and opacity of ice. While not evaluated here, the rate of melt can have important consequences for tree branches and electrical transmission wires that are subjected to windy conditions after storms (Jones et al. 2002) as this affects ice unloading and secondary failure potential. Because weather can change rapidly after storms, it is important to make measurements soon after the storm ends. Making supplemental measurements of ice thickness regularly in the days and weeks that follow the storm can provide additional information, such as interactive effects of wind and ice.

d. Measurement position

For both wires and rods, vertical ice accretion measurements were significantly greater than horizontal measurements, indicating that more ice accumulated on the top and bottom of the wires and rods compared to the sides. With the caliper measurement method we used, it was not possible to determine how much ice accumulated on the top of the rod or wire compared to the bottom or if one side accumulated more than the other. However, based on visual inspections after the ice

applications it appeared that more ice had accumulated on top of the rods. These results confirm the importance of making both horizontal and vertical measurements for determining ice loads on wires and rods, as the uniformity of ice on structures can be highly variable depending on weather conditions (Poots 1996; Jones and Mulherin 1998; Makkonen 1998).

For plates, there was no significant difference in ice accretion among the three locations on the collectors where measurements were made, indicating that the ice was distributed evenly over the surface. There was also no significant difference in ice accretion among the three locations along wires where measurements were made, although the *p* value was low (*p* = 0.099) and mean ice thickness in the center position on wires was greater than on either side. The bare wires were taut, but sagged with ice load, possibly causing the freezing rain to flow toward the lowest point on the wire. For rods installed horizontally and at 60°, there was no significant difference in ice accretion among the three measurement locations (Fig. 7). However, rods that were installed at a 30° angle had more ice accumulation toward the base of the rod, indicating a tendency for the water to flow downward before freezing. It is surprising that this pattern was not evident for rods installed at a 60° angle; however, rods at this inclination had significantly less ice, perhaps because the steeper angle caused unfrozen precipitation to shed off the collector rather than accumulate as ice toward the base. Our results suggest that for collectors mounted horizontally, it is not critical to make measurements in the exact same location on the collector. However, the nonuniformity of ice on rods mounted at a 30° angle requires horizontal and vertical measurements at fixed intervals along the length of the rod, that can be used to calculate an average value for the rod.

As stated previously, rods mounted at a 60° angle had less ice than rods mounted at 0° and 30° (Fig. 5a). At the lower level of icing, there was no significant difference in ice accretion between rods at 0° and 30°, but at the higher level of icing, more ice accumulated on rods installed at 30°. Icicles formed on rods installed horizontally and measurements were made in-between icicles so as not to inflate the ice thickness values. Rods installed at 30° had little to no icicles and did not shed the freezing water like rods installed at 60°. Previous studies have overcome issues with icicles by measuring the volume of meltwater from the collector and calculating radial ice thickness using an assumed ice density. This method has been applied to tree limbs (Jones and Mulherin 1998) and wooden dowels (Rustad and Campbell 2012) that were destructively sampled with ice on them, as well as removable rods that can be reused (Ryerson and

Ramsay 2007). Relative to caliper measurements, methods based on ice mass may provide a better estimate of ice accretion when ice formation is irregular. However, caliper measurements require less effort and equipment, making them more practical for volunteer observers. The quality of calipers can vary widely, with prices ranging from several dollars to thousands of dollars. We used relatively inexpensive digital calipers in this study (~\$25), but even less expensive analog calipers could be used and likely provide better measurements than a ruler.

e. Uncertainty analysis

Reproducibility of measurements was assessed by repeating measurements at the higher level of icing using the same methods and under the same conditions, but with different technicians. Results of this analysis showed a slight positive bias (0.4%–1.6%; Table 1), indicating that measurements from one technician were slightly different than the other. This bias could be due to differences in the skill of the technicians making measurements. For example, calipers can expand slightly as they are being removed from the ice or if they are not held at the proper angle, resulting in a positive bias. Although the bias was small, it highlights the importance of proper training to minimize these effects. The reproducibility was greatest on plates and lowest on wires, with rods being intermediate. Some of the error can be attributed to icicles, which were removed from plates, and formed mostly on wires and rods that were oriented horizontally. Precision for rods installed horizontally was 6.3% as compared with rods installed at 30° (4.9%) and 60° (4.8%). The poorer precision for wires is mostly attributed to the rougher surface of the stranded wire. Precision for the bare aluminum stranded wire was 13.3% as compared with 6.7% for the smoother insulated wire. Thus, ice measurements on collectors with a smooth surface have higher precision.

5. Conclusions and future research needs

The ice-storm simulation successfully generated two realistic levels of ice accretion for evaluating low-cost, passive ice collector configurations. Although the amount and uniformity of ice would be expected to vary under different weather conditions, the simulation provided insight about how collector types and their attributes affect measurements. As anticipated, collectors made of rods accumulated significantly less ice than plates, highlighting the need for detailed reporting of the methods used to measure ice accretion. Precision of measurements on bare stranded wires was lower than other collector types due to the irregular surface. Icicles were removed from plates before measurement but formed on wires and

rods installed horizontally. When icicles were present, caliper measurements underestimated ice accretion because measurements were made between icicles. Icicles did not form on rods installed at a 30° angle, but at a greater incline (i.e., 60°) unfrozen precipitation shed off the collectors, resulting in lower estimates.

Ice accretion can be determined in many ways, and all methods have advantages and disadvantages. Manual measurements of ice thickness are reliable and inexpensive but labor intensive. Automated freezing-rain sensors have become prevalent in recent years, and the technology will continue to improve and become more affordable in the future. Currently there is a pressing need to make observations of ice accretion using a variety of approaches at the same location. While we evaluated differences among several types of passive ice collectors in this study, it would be advantageous to incorporate other methods, including various automated sensors, in future research. This comparison would help to characterize differences among collectors and enable development of conversion factors. Establishing relationships among measurement methods will provide critical data for modeling and mapping ice accretion and ultimately a more accurate quantitative understanding of ice-storm impacts on ecosystems, infrastructure, and society.

Acknowledgments. Funding for this research was provided by the National Science Foundation (DEB-1457675) and U.S. Department of Agriculture (USDA) Forest Service. We thank Clara Chaisson, Brendan Leonard, Mary Martin, Hannah Vollmer, Gabe Winant, and David Zietlow for help with fieldwork. This paper is a contribution of the Hubbard Brook Ecosystem Study. Hubbard Brook is part of the Long-Term Ecological Research (LTER) network, which is supported by the National Science Foundation (DEB-1633026). The Hubbard Brook Experimental Forest is operated and maintained by the USDA Forest Service, Northern Research Station, Newtown Square, Pennsylvania.

REFERENCES

Ackley, S. F., and M. K. Templeton, 1979: Computer modeling of atmospheric ice accretion. CRREL Rep. 79-4, 39 pp.

American Meteorological Society, 2020: Drizzle. *Glossary of Meteorology*, accessed 2 March 2020, <http://glossary.ametsoc.org/wiki/Drizzle>.

Bennett, I., 1959: Glaze: Its meteorology and climatology, geographical distribution, and economic effects. Quartermaster Research and Engineering Center Tech. Rep. EP-15, 234 pp.

Call, D. A., 2010: Changes in ice storm impacts over time: 1886–2000. *Wea. Climate Soc.*, **2**, 23–35, <https://doi.org/10.1175/2009WCAS1013.1>.

Campbell, J., 2016: Hubbard Brook Experimental Forest: Daily mean temperature data, 1955–present. Environmental Data Initiative, accessed 7 February 2020, <https://doi.org/10.6073/pasta/5885076607dd57101dfd6129758d5adc>.

Changnon, S. A., 2003: Characteristics of ice storms in the United States. *J. Appl. Meteor.*, **42**, 630–639, [https://doi.org/10.1175/1520-0450\(2003\)042<0630:COISIT>2.0.CO;2](https://doi.org/10.1175/1520-0450(2003)042<0630:COISIT>2.0.CO;2).

—, and T. G. Creech, 2003: Sources of data on freezing rain and resulting damages. *J. Appl. Meteor.*, **42**, 1514–1518, [https://doi.org/10.1175/1520-0450\(2003\)042<1514:SODOFR>2.0.CO;2](https://doi.org/10.1175/1520-0450(2003)042<1514:SODOFR>2.0.CO;2).

—, and T. R. Karl, 2003: Temporal and spatial variations of freezing rain in the contiguous United States: 1948–2000. *J. Appl. Meteor.*, **42**, 1302–1315, [https://doi.org/10.1175/1520-0450\(2003\)042<1302:TASVOF>2.0.CO;2](https://doi.org/10.1175/1520-0450(2003)042<1302:TASVOF>2.0.CO;2).

Cifelli, R., N. Doesken, P. Kennedy, L. D. Carey, S. A. Rutledge, C. Gimmetad, and T. Depue, 2005: The Community Collaborative Rain, Hail, and Snow network: Informal education for scientists and citizens. *Bull. Amer. Meteor. Soc.*, **86**, 1069–1078, <https://doi.org/10.1175/BAMS-86-8-1069>.

Cortinas, J. V., Jr., B. C. Bernstein, C. C. Robbins, and J. W. Strapp, 2004: An analysis of freezing rain, freezing drizzle, and ice pellets across the United States and Canada: 1976–90. *Wea. Forecasting*, **19**, 377–390, [https://doi.org/10.1175/1520-0434\(2004\)019<0377:AAOFRF>2.0.CO;2](https://doi.org/10.1175/1520-0434(2004)019<0377:AAOFRF>2.0.CO;2).

DeGaetano, A. T., 2000: Climatic perspectives and impacts of the 1998 northern New York and New England ice storm. *Bull. Amer. Meteor. Soc.*, **81**, 237–254, [https://doi.org/10.1175/1520-0477\(2000\)081<0237:CPAIOT>2.3.CO;2](https://doi.org/10.1175/1520-0477(2000)081<0237:CPAIOT>2.3.CO;2).

Fan, C., and X. Jiang, 2018: Analysis of the icing accretion performance of conductors and its normalized characterization method of icing degree for various ice types in natural environments. *Energies*, **11**, 2678, <https://doi.org/10.3390/en1102678>.

Fikke, S., and Coauthors, 2006: COST 727: Atmospheric icing on structures—Measurements and data collection on icing: State of the Art. MeteoSwiss Publ. 75, 110 pp., https://www.wmo.int/pages/prog/www/IMOP/meetings/Surface/ET-STMT-2/COST-727-report_MCH-V75.pdf.

Fu, P., M. Farzaneh, and G. Bouchard, 2006: Two-dimensional modelling of the ice accretion process on transmission line wires and conductors. *Cold Reg. Sci. Technol.*, **46**, 132–146, <https://doi.org/10.1016/j.coldregions.2006.06.004>.

Gay, D. A., and R. E. Davis, 1993: Freezing rain and sleet climatology of the southeastern USA. *Climate Res.*, **3**, 209–220, <https://doi.org/10.3354/cr003209>.

Groisman, P. Ya., O. N. Bulygina, X. Yin, R. S. Vose, S. K. Gulev, I. Hanssen-Bauer, and E. Førland, 2016: Recent changes in the frequency of freezing precipitation in North America and northern Eurasia. *Environ. Res. Lett.*, **11**, 045007, <https://doi.org/10.1088/1748-9326/11/4/045007>.

Gyakum, J. R., and P. J. Roeber, 2001: The 1998 Ice Storm—Analysis of a planetary-scale event. *Mon. Wea. Rev.*, **129**, 2983–2997, [https://doi.org/10.1175/1520-0493\(2001\)129<2983:TISAOA>2.0.CO;2](https://doi.org/10.1175/1520-0493(2001)129<2983:TISAOA>2.0.CO;2).

Homola, M. C., P. J. Nicklason, and P. A. Sundsbø, 2006: Ice sensors for wind turbines. *Cold Reg. Sci. Technol.*, **46**, 125–131, <https://doi.org/10.1016/j.coldregions.2006.06.005>.

Houlton, B. Z., C. T. Driscoll, T. J. Fahey, G. E. Likens, P. M. Groffman, E. S. Bernhardt, and D. C. Buso, 2003: Nitrogen dynamics in ice storm-damaged forest ecosystems: Implications for nitrogen limitation theory. *Ecosystems*, **6**, 431–443, <https://doi.org/10.1007/s10021-002-0198-1>.

Huffman, G. J., and G. A. Norman, 1988: The supercooled warm rain process and the specification of freezing precipitation. *Mon. Wea.*

Rev., **116**, 2172–2182, [https://doi.org/10.1175/1520-0493\(1988\)116<2172:TSWRPA>2.0.CO;2](https://doi.org/10.1175/1520-0493(1988)116<2172:TSWRPA>2.0.CO;2).

Hyslop, N. P., and W. H. White, 2009: Estimating precision using duplicate measurements. *J. Air Waste Manage. Assoc.*, **59**, 1032–1039, <https://doi.org/10.3155/1047-3289.59.9.1032>.

Irland, L. C., 1998: Ice storm 1998 and the forests of the Northeast: A preliminary assessment. *J. For.*, **96**, 32–40, <https://doi.org/10.1093/jof/96.9.32>.

—, 2000: Ice storms and forest impacts. *Sci. Total Environ.*, **262**, 231–242, [https://doi.org/10.1016/S0048-9697\(00\)00525-8](https://doi.org/10.1016/S0048-9697(00)00525-8).

ISO, 2017: Atmospheric icing of structures. International Organization for Standardization ISO Standard 12494, 58 pp., <https://www.iso.org/standard/72443.html>.

Jones, K. F., 1996: Ice accretion in freezing rain. CRREL Rep. 96-2, 23 pp., <https://apps.dtic.mil/dtic/tr/fulltext/u2/a310659.pdf>.

—, 1998: A simple model for freezing rain ice loads. *Atmos. Res.*, **46**, 87–97, [https://doi.org/10.1016/S0169-8095\(97\)00053-7](https://doi.org/10.1016/S0169-8095(97)00053-7).

—, and N. D. Mulherin, 1998: An evaluation of the severity of the January 1998 ice storm in northern New England. U.S. Army Corps of Engineers FEMA Region 1 Rep., 66 pp.

—, R. Thorikildson, and J. N. Lott, 2002: The development of a U.S. climatology of extreme ice loads. NOAA National Climatic Data Center Tech. Rep. 2002-01, 23 pp., [https://doi.org/https://doi.org/10.1061/40642\(253\)2](https://doi.org/https://doi.org/10.1061/40642(253)2).

Kramer, C. Y., 1956: Extension of multiple range tests to group means with unequal numbers of replications. *Biometrics*, **12**, 307–310, <https://doi.org/10.2307/3001469>.

Laflamme, J., 1995: Spatial variation of extreme values for freezing rain. *Atmos. Res.*, **36**, 195–206, [https://doi.org/10.1016/0169-8095\(94\)00035-C](https://doi.org/10.1016/0169-8095(94)00035-C).

Laforte, J. L., M. A. Allaire, and J. Laflamme, 1998: State-of-the-art on power line de-icing. *Atmos. Res.*, **46**, 143–158, [https://doi.org/10.1016/S0169-8095\(97\)00057-4](https://doi.org/10.1016/S0169-8095(97)00057-4).

Landolt, S. D., J. S. Lave, D. Jacobson, A. Gaydos, S. DiVito, and D. Porter, 2019: The impacts of automation on present weather-type observing capabilities across the conterminous United States. *J. Appl. Meteor. Climatol.*, **58**, 2699–2715, <https://doi.org/10.1175/JAMC-D-19-0170.1>.

Levene, H., 1960: Robust tests for equality of variances. *Contributions to Probability and Statistics*, I. Olkin, Ed., Stanford University Press, 278–292.

Likens, G. E., B. K. Dresser, and D. C. Buso, 2004: Short-term temperature response in forest floor and soil to ice storm disturbance in a northern hardwood forest. *North. J. Appl. For.*, **21**, 209–219, <https://doi.org/10.1093/njaf/21.4.209>.

Makkonen, L., 1998: Modeling power line icing in freezing precipitation. *Atmos. Res.*, **46**, 131–142, [https://doi.org/10.1016/S0169-8095\(97\)00056-2](https://doi.org/10.1016/S0169-8095(97)00056-2).

—, 2000: Models for the growth of rime, glaze, icicles and wet snow on structures. *Philos. Trans. Roy. Soc. London*, **358A**, 2913–2939, <https://doi.org/10.1098/rsta.2000.0690>.

—, and J. R. Stallabrass, 1987: Experiments on the cloud droplet collision efficiency of cylinders. *J. Climate Appl. Meteor.*, **26**, 1406–1411, [https://doi.org/10.1175/1520-0450\(1987\)026<1406:EOTCDC>2.0.CO;2](https://doi.org/10.1175/1520-0450(1987)026<1406:EOTCDC>2.0.CO;2).

McComber, P., 1983: Numerical simulation of ice accretion on cables. *First Int. Workshop on Atmospheric Icing of Structures*, CRREL Special Rep. 83-17, 51–58.

Mughal, U. N., M. Virk, and M. Y. Mustafa, 2016: State of the art review of atmospheric icing sensors. *Sens. Transducers*, **198**, 2–15.

Myers, T. G., and J. P. F. Charpin, 2004: A mathematical model for atmospheric ice accretion and water flow on a cold surface. *Int. J. Heat Mass Transf.*, **47**, 5483–5500, <https://doi.org/10.1016/j.ijheatmasstransfer.2004.06.037>.

Nagel, T. A., D. Firm, D. Rozenbergar, and M. Kobal, 2016: Patterns and drivers of ice storm damage in temperate forests of central Europe. *Eur. J. For. Res.*, **135**, 519–530, <https://doi.org/10.1007/s10342-016-0950-2>.

NWS, 2019: WFO Winter Weather Products Specification. National Weather Service Instruction 10-513, 50 pp., <https://www.nws.noaa.gov/directives/sym/pd01005013curr.pdf>.

Poots, G., 1996: *Ice and Snow Accretion on Structures*. John Wiley and Sons, 338 pp.

Rauber, R. M., L. S. Olthoff, M. K. Ramamurthy, and K. E. Kunkel, 2000: The relative importance of warm rain and melting processes in freezing precipitation events. *J. Appl. Meteor.*, **39**, 1185–1195, [https://doi.org/10.1175/1520-0450\(2000\)039<1185:TRIOWR>2.0.CO;2](https://doi.org/10.1175/1520-0450(2000)039<1185:TRIOWR>2.0.CO;2).

—, —, —, D. Miller, and K. E. Kunkel, 2001: A synoptic weather pattern and sounding-based climatology of freezing precipitation in the United States east of the Rocky Mountains. *J. Appl. Meteor.*, **40**, 1724–1747, [https://doi.org/10.1175/1520-0450\(2001\)040<1724:ASWPAS>2.0.CO;2](https://doi.org/10.1175/1520-0450(2001)040<1724:ASWPAS>2.0.CO;2).

Reges, H. W., N. Doesken, J. Turner, N. Newman, A. Bergantino, and Z. Schwalbe, 2016: CoCoRaHS: The evolution and accomplishments of a volunteer rain gauge network. *Bull. Amer. Meteor. Soc.*, **97**, 1831–1846, <https://doi.org/10.1175/BAMS-D-14-00213.1>.

Rhoads, A. G., and Coauthors, 2002: Effects of an intense ice storm on the structure of a northern hardwood forest. *Can. J. For. Res.*, **32**, 1763–1775, <https://doi.org/10.1139/x02-089>.

Rustad, L. E., and J. L. Campbell, 2012: A novel ice storm manipulation experiment in a northern hardwood forest. *Can. J. For. Res.*, **42**, 1810–1818, <https://doi.org/10.1139/x2012-120>.

Ryerson, C. C., and A. C. Ramsay, 2007: Quantitative ice accretion information from the automated surface observing system. *J. Appl. Meteor. Climatol.*, **46**, 1423–1437, <https://doi.org/10.1175/JAM2535.1>.

Sanders, K. J., and B. L. Barjenbruch, 2016: Analysis of ice-to-liquid ratios during freezing rain and the development of an ice accumulation model. *Wea. Forecasting*, **31**, 1041–1060, <https://doi.org/10.1175/WAF-D-15-0118.1>.

SAS Institute, 2012: SAS Version 9.4. SAS Institute, Inc.

Shapiro, S. S., and M. B. Wilk, 1965: An analysis of variance test for normality (complete samples). *Biometrika*, **52**, 591–611, <https://doi.org/10.1093/biomet/52.3-4.591>.

Smith, A. B., and R. W. Katz, 2013: US billion-dollar weather and climate disasters: Data sources, trends, accuracy and biases. *Nat. Hazards*, **67**, 387–410, <https://doi.org/10.1007/s11069-013-0566-5>.

Stewart, R. E., and P. King, 1987: Freezing precipitation in winter storms. *Mon. Wea. Rev.*, **115**, 1270–1280, [https://doi.org/10.1175/1520-0493\(1987\)115<1270:FPIWS>2.0.CO;2](https://doi.org/10.1175/1520-0493(1987)115<1270:FPIWS>2.0.CO;2).

Szilder, K., 2018: Theoretical and experimental study of ice accretion due to freezing rain on an inclined cylinder. *Cold Reg. Sci. Technol.*, **150**, 25–34, <https://doi.org/10.1016/j.coldregions.2018.02.004>.

Tattelman, P., 1982: An objective method for measuring surface ice accretion. *J. Appl. Meteor.*, **21**, 599–612, [https://doi.org/10.1175/1520-0450\(1982\)021<0599:AOMFMS>2.0.CO;2](https://doi.org/10.1175/1520-0450(1982)021<0599:AOMFMS>2.0.CO;2).

Tobin, D. M., M. R. Kumjian, and A. W. Black, 2019: Characteristics of recent vehicle-related fatalities during active precipitation in the United States. *Wea. Climate Soc.*, **11**, 935–952, <https://doi.org/10.1175/WCAS-D-18-0110.1>.

USDA Forest Service, Northern Research Station, 2019: Hubbard Brook Experimental Forest: Daily precipitation standard rain gage measurements, 1956–present. Environmental Data Initiative, accessed 7 February 2020, <https://doi.org/10.6073/pasta/c9dc21212a3af50216f2db706f059714>.

Virk, M. S., 2017: Ice accretion on circular cylinder in relation to its diameter. *Wind Eng.*, **41**, 55–61, <https://doi.org/10.1177/0309524X16675247>.

—, M. Y. Mustafa, and Q. Hamdan, 2011: Atmospheric ice accretion measurement techniques. *Int. J. Multiphys.*, **5**, 229–241, <https://doi.org/10.1260/1750-9548.5.3.229>.

—, U. M. Mughal, and G. Polanco, 2015: Atmospheric ice accretion on non-rotating vertical circular cylinder. *World J. Eng. Technol.*, **3**, 284–289, <https://doi.org/10.4236/wjet.2015.33C042>.

Zarnani, A., P. Musilek, X. Shi, X. Ke, H. He, and R. Greiner, 2012: Learning to predict ice accretion on electric power lines. *Eng. Appl. Artif. Intell.*, **25**, 609–617, <https://doi.org/10.1016/j.engappai.2011.11.004>.

Zhou, B., and Coauthors, 2011: The great 2008 Chinese ice storm: Its socioeconomic–ecological impact and sustainability lessons learned. *Bull. Amer. Meteor. Soc.*, **92**, 47–60, <https://doi.org/10.1175/2010BAMS2857.1>.